Imaging three-dimensional surface objects with submolecular resolution by atomic force microscopy

(Supporting Information)

César Moreno,[*,†,‡,‖] Oleksandr Stetsovych,[†,¶] Tomoko K. Shimizu,[†,§] and Oscar Custance[†]

National Institute for Materials Science (NIMS), 1-2-1 Sengen, 305-0047 Tsukuba, Ibaraki, Japan, International Center for Young Scientists, NIMS, 1-2-1 Sengen, 305-0047 Tsukuba, Ibaraki, Japan, Institute of Physics, Academy of Sciences of the Czech Republic, Cukrovarnicka 10, Prague, Czech Rebublic, and JST, PRESTO, 4-1-8 Honcho, Kawaguchi, Saitama, 332-0012, Japan

E-mail: cesar.moreno@icn.cat

[*]To whom correspondence should be addressed

[†]National Institute for Materials Science (NIMS), 1-2-1 Sengen, 305-0047 Tsukuba, Ibaraki, Japan

[‡]International Center for Young Scientists, NIMS, 1-2-1 Sengen, 305-0047 Tsukuba, Ibaraki, Japan

[¶]Institute of Physics, Academy of Sciences of the Czech Republic, Cukrovarnicka 10, Prague, Czech Rebublic

[§]JST, PRESTO, 4-1-8 Honcho, Kawaguchi, Saitama, 332-0012, Japan

[‖]Current address: Catalan Institute of Nanoscience and Nanotechnology (ICN2), 08193 Bellaterra, Barcelona, Spain

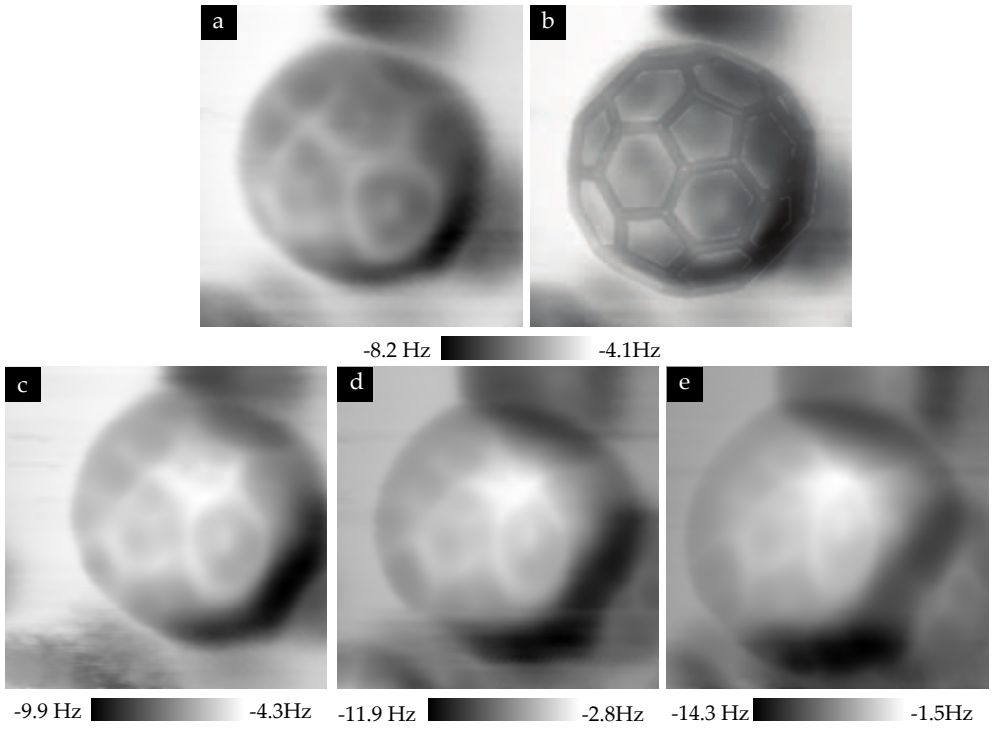

Figure S1: **Intramolecular resolution images of a C_{60} molecule at several probe-surface separation distances.** **a**, Δf image shown in Fig. 2b. **b**, Same image as in (a) with a structural model of the C_{60} molecule superimposed. The direct comparison between the model and the intra-molecular resolution image enables to assess the adsorption geometry of the C_{60} molecule displayed in Figs. 2a to 2c. **c**, **d** and **e**, Δf images of the same C_{60} molecule but measured by applying an offset distance towards the surface of 0.3 nm, 0.35 nm and 0.4 nm, respectively, for the second line scan with respect to the topography measured during the first line scans. When further approaching the probe towards the surface during the second line scans with respect to the optimum imaging separation, the deformation of the molecule and the blurring of the intramolecular features are obtained. If the probe termination is not atomically sharp the features imaged during the second pass could also suffer from dilation. Acquisition parameters and image dimensions are the same as for Fig. 2.

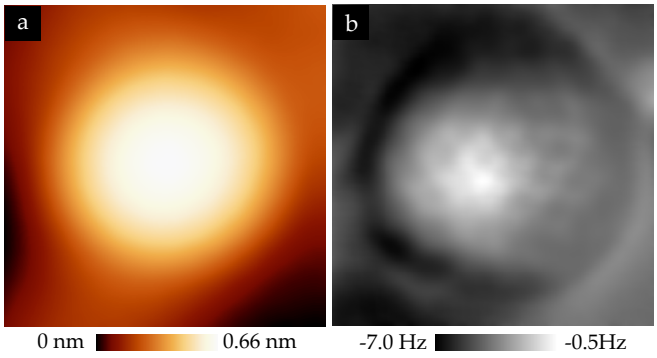

Figure S2: **Intramolecular resolution imaging with a C_{60} molecules at the probe apex**. **a**, Topographic image of a C_{60} molecule deposited on the (101) anatase surface obtained by applying the multi-pass method described in the text. **b**, Δf signal recorded during the second line scans. The distance offset for the second line scans was 0.25 nm towards the surface with respect to the topography measured during the first line scans. Image dimensions are (3×3) nm^2. These images were acquired after picking up C_{60} molecules from the surface. Most likely, the golf-ball-like features displayed by the Δf image are the result of the convolution of localised molecule-molecule interactions. Acquisition parameters are: f= 159200 Hz; A= 179.5 Å ; K= 26.9 N·m^{-1}; V_{CPD}= -300 mV. The topographic set point value for the first line scans was Δf= -2.0 Hz, and the second line scans were carried out by approaching the probe 0.19 nm towards the surface with respect to the topography recorded during the first line scans.

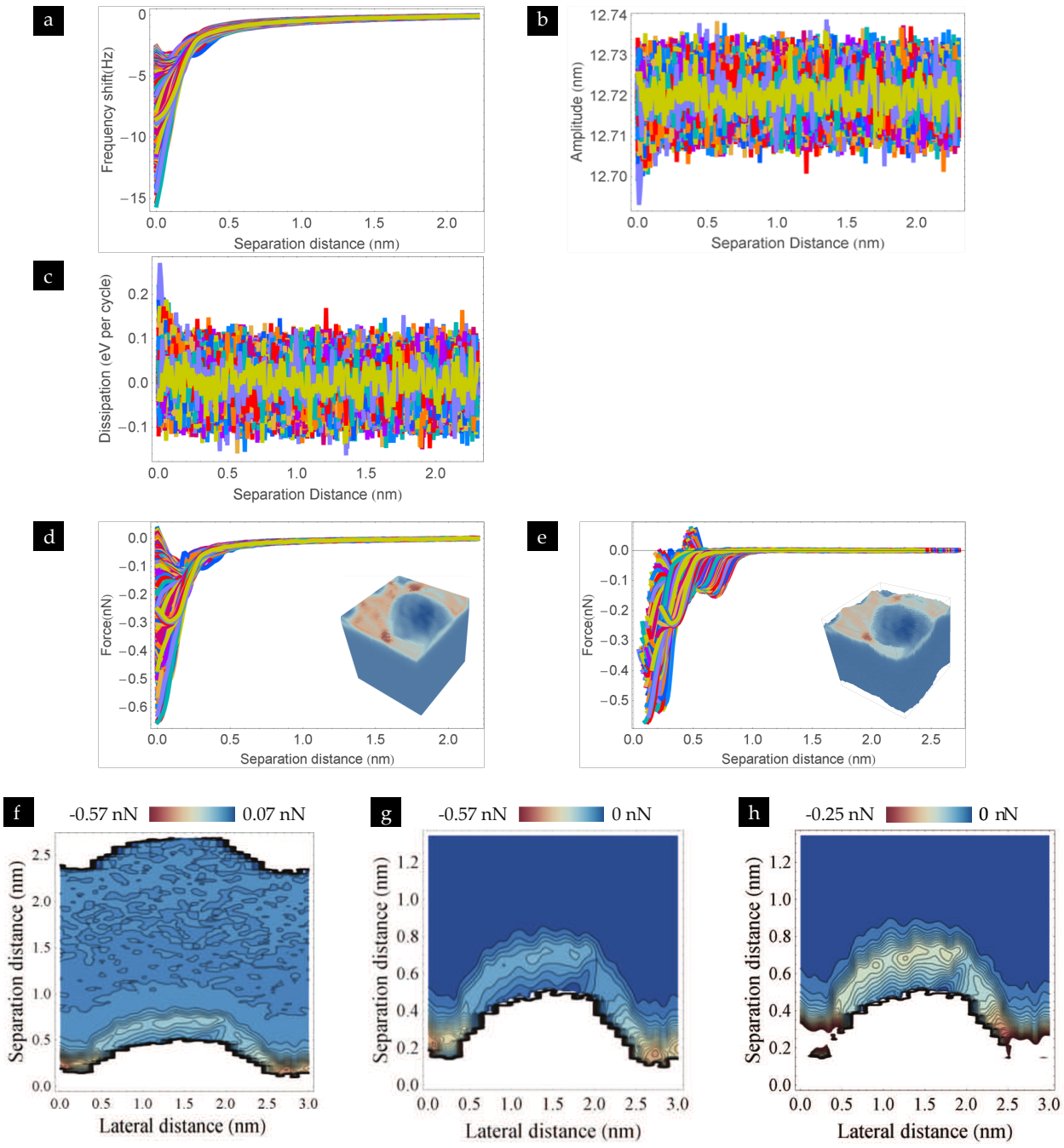

Figure S3: **Force volume spectroscopy data.** **a**, Frequency shift versus tip-surface separation distance curves. **b**, Amplitude and **c**, dissipation signals simultaneously recorded with the frequency shift curves in (a). **d**, Total force curves and rendered force volume derived from these curves (inset). Force spectroscopy data is composed by 36 × 36 curves with 256 points per curve. The colour scale spans from 0.03 nN (blue) to -0.65 nN (red). **e**, Short-range force curves obtained after the subtraction of a fit to the long-range contribution to the total interaction force and the correction of topographic effects derived from the stabilization of the probe-surface separation in closed feedback loop between the acquisition of consecutive curves. The inset shows the corresponding rendered force volume. **f**, Force map shown in Fig. 2e represented with full tip-surface separation distance and interaction force scale. **g**, Force map displayed in Fig. 2e with wider tip-surface interaction force scale. **h**, Force map in Fig. 2e for comparison with (f) and (g).

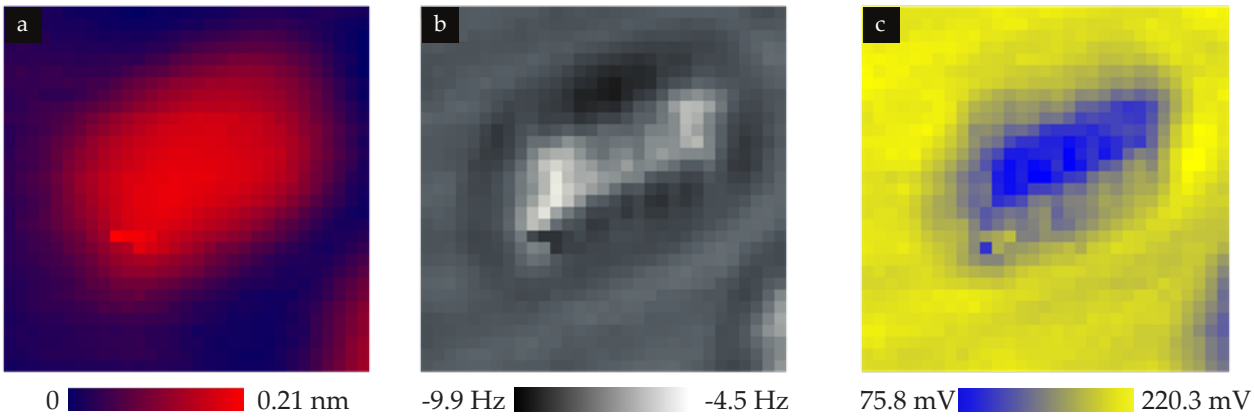

Figure S4: **Variation of the local contact potential difference over the pentacene molecule shown in Fig. 1**. In all the experiments reported in this work, the long-range electrostatic interaction was spatially homogeneous at the typical separation distances at which the first line scans were performed, and its force value was approximately a hundred times smaller than the van der Waals contribution at the same probe-surface separation. Upon this situation, a fair minimization of the long-range electrostatic interaction force is accomplished by compensating the probe-surface contact potential difference one or two nanometers away from the surface.[1] At closer tip-surface separations, the local contact potential difference values detected in these experiments are comparable to the ones recorded over polar and bipolar individual molecules reported in B. Schuler *et al.*,[2] as it is shown in this figure. **a**, Topographic image measured at the same probe-surface separation as for Fig. 1b obtained from the stabilization of the tip-sample distance during the acquisition of a bias-spectroscopy imaging measurement.[1] For each of the (32x32) pixels of the image, the topographic feedback was set to the separation at which the first line scans were performed (Δf= -4.5 Hz), the feedback loop was then opened and the tip was brought closer to the surface the same distance as for the second line scans (d= 0.3 nm). A frequency shift vs. bias voltage [Δf(V)] curve was then acquired, the tip was retracted from the surface, and the topographic feedback was activated again before moving the probe to the next pixel of the image. Each of these Δf(V) curves was fitted to a quadratic function to obtain the peak voltage and the corresponding Δf values that locally minimises the electrostatic interaction (the local contact potential difference is this peak voltage value divided by the electron charge). **b** Map of the Δf that minimises the electrostatic interaction measured at the same tip-surface separation as in Fig. 1c. **c** , Map of the local contact potential difference obtained at the same tip-surface separation as in Fig. 1c. The images are slightly deformed with respect to the images in Fig. 1 due to thermal drift, because the acquisition time for this bias-spectroscopy imaging measurement was considerably longer than for the images shown in Fig. 1. Acquisition parameters and image dimensions are the same as for Fig. 1. In the hypothetical case of detecting a strong and non homogeneous distribution of the long-range electrostatic force at the tip-surface separation at which the first line scans are performed (as well as for closer probe-surface separation distances), high-resolution imaging using the multi-pass method reported in the main text may require minimisation of the electrostatic interaction by instantaneous compensation of the local contact potential difference by a Kelvin probe microscopy controller, for example.

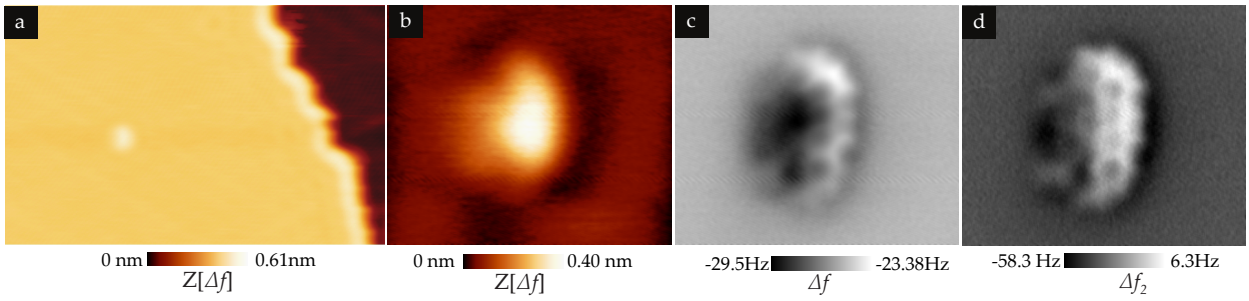

Figure S5: **Submolecular resolution of a pentacene molecule on a Cu(111) surface.a**, Topographic (Z[Δf]) image of a Cu(111) terrace showing a pentacene molecule pinned to a defect site (protrusion at the center of the terrace). Image dimensions are (30 × 19) nm^2. **b**, Topographic image associated with the first line scans over the pentacene molecule shown in (a). **c** and **d**, Images of the variation of the resonant frequency of the first (Δf) and second (Δf_2) cantilever longitudinal flexural modes, respectively, acquired simultaneously as the image in (b) but during the second line scans. The offset distance the probe was approached towards the surface during the second line scan was 0.22 nm. Image dimensions are (3 × 2.6) nm^2. The topographic set point for the first line scans is Δf= -19 Hz. In this experiment, a pristine Pt-Ir cantilever tip was used. The tip was Ar-ion sputtered after insertion in UHV environment, and in-situ tip conditioning on the Cu(111) surface was performed by following the procedure described in the *Methods* section until good AFM sensitivity to short-range forces was obtained. Pentacene is mobile on Cu(111) even at 55K.[3] The fact that the pentacene molecule shown in these images is firmly anchored to the substrate may be a reason behind the possibility of obtaining intra-molecular resolution with a metallic tip. Alternatively, the apex of the probe could be contaminated with other pentacene molecules. In this case, however, we would expect diffusion of the molecules also at the probe apex that would develop into instabilities during imaging. These images demonstrate that the method reported here can also provide high-resolution images of adsorbates deposited on metallic substrates.

References

(1) Sadewasser, S.; Jelinek, P.; Fang, C.-K.; Custance, O.; Yamada, Y.; Sugimoto, Y.; Abe, M.; Morita, S. *Phys. Rev. Lett.* **2009**, *103*, 266103.

(2) Schuler, B.; Liu, S.-X.; Geng, Y.; Decurtins, S.; Meyer, G.; Gross, L. *Nano Lett.* **2014**, *14*, 3342–3346.

(3) Smerdon, J. A.; Bode, M.; Guisinger, N. P.; Guest, J. R. *Phys. Rev. B* **2011**, *84*, 165436.